$R_3C-H\rightarrow SiFR_3$ Agostic Interaction

Christopher L. Dorsey and François P. Gabbaï*

Department of Chemistry, Texas A&M University, College Station, Texas 77843

Received March 20, 2008

As part of our investigations of main group complexes with unusual bridging interactions, we have set out to determine if fluorosilane Lewis acids could form σ-complexes with alkanes. In order to probe this possibility, we have synthesized the cationic fluorosilane 1-(dimethylfluorosilane)-8-(9-xanthylium)naphthalenediyl ([**2**]$^+$) as a tetrafluoroborate salt and converted it into 1-(dimethylfluorosilane)-8-(9*H*-xanthene)naphthalenediyl (**3**) by reaction with $NaBH_4$. Both [**2**][BF_4] and **3** have been fully characterized. Examination of the structure of **3** indicates the presence of an interaction involving the C−H bond at the 9-position of the xanthene unit and the silicon atom. This interaction, which is characterized by a Si−H separation of 2.32(2) Å and a F−Si−H angle of 177.0(5)°, leads the silicon atom to adopt a distorted trigonal-bipyramidal geometry. The nature of this interaction has been investigated experimentally by NMR and IR spectroscopy as well as computationally using density functional calculations, atom in molecules, and natural bond order analyses. These combined experimental and computational results suggest that the short Si−H contact in **3** corresponds to an agostic C−H → Si interaction.

Introduction

Fluorosilanes are Lewis acidic derivatives that can expand their coordination sphere to accept a Lewis basic ligand.[1–4] Formation of the ensuing pentacoordinate silicon species is a result of electron donation from a filled orbital of the donor into the σ^*-orbital of the Si−F bond.[5] In the case of triorganylfluorosilanes, most Lewis adducts usually involve hard anionic ligands such as fluoride[6,7] or alkoxide anions.[8] Complexes featuring neutral donors are in fact much more scarce and usually feature a neutral Lewis basic atom such as nitrogen coordinated to the silicon atom in an intramolecular fashion.[9–12] Complexes with weaker donors have remained highly elusive. For example, fluorosilane σ-complexes involving an alkane as a donor have never been considered, although silylium ions have been shown to engage in α-agostic C−H interactions.[13]

The naphthalene backbone has often been used as a scaffold for the stabilization of unusual bridging interactions. In particular, species featuring $[R_3C-H \rightarrow CR_3]^+$ ([**Ia**−**c**]$^+$),[14,15] $[R_3C-F \rightarrow CR_3]^+$ ([**II**]$^+$),[16] $[R_3Si-H-SiR_3]^+$ ([**III**]$^+$),[17] and $[R_3Si-F-SiR_3]^+$ ([**IV**]$^+$)[17] bridging motifs have been described recently (Chart 1). In this paper, we now report the synthesis and characterization of a *peri*-substituted naphthalene derivative that features an agostic $R_3C-H \rightarrow SiFR_3$ σ-interaction.

Chart 1

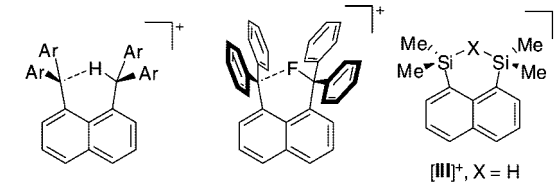

[**Ia-c**]$^+$ [**II**]$^+$ [**III**]$^+$, X = H; [**IV**]$^+$, X = F

a: Ar_2C^+ = 10-methyl-9-acridinium
b: Ar = C_6H_5
c: Ar = *p*-C_6H_4OMe

Experimental Section

General Considerations. 1,8-Dilithionaphthalene was prepared following a published procedure. THF was dried by refluxing over Na/K under a N_2 atmosphere. Air-sensitive compounds were handled under a N_2 atmosphere using standard Schlenk and glovebox techniques. Elemental analyses were performed at Atlantic Microlab (Norcross, GA). All melting points were measured on samples in sealed capillaries and are uncorrected. NMR spectra were recorded on a Varian Unity Inova 400 FT NMR (399.59 MHz for ^{1}H, 375.99 MHz for ^{19}F, 100.47 MHz for ^{13}C, and 79.39 for ^{29}Si) and a Varian Inova 500 FT NMR (499.95 MHz for ^{1}H and 125.71 MHz for ^{13}C). Chemical shifts δ are given in ppm and are

* Corresponding author. E-mail: francois@tamu.edu.

(1) Chuit, C.; Corriu, R. J. P.; Reye, C.; Young, J. C. *Chem. Rev.* **1993**, *93*, 1371.
(2) Holmes, R. R. *Chem. Rev.* **1990**, *90*, 17.
(3) Voronkov, M. G.; Gubanova, L. I. *Main Group Met. Chem.* **1987**, *10*, 210.
(4) Tamao, K.; Hayashi, T.; Ito, Y. *J. Organomet. Chem.* **1996**, *506*, 85.
(5) Schoeller, W. W.; Rozhenko, A. *Eur. J. Inorg. Chem.* **2000**, 375.
(6) Yamaguchi, S.; Akiyama, S.; Tamao, K. *J. Am. Chem. Soc.* **2000**, *122*, 6335.
(7) Tamao, K.; Hayashi, T.; Ito, Y.; Shiro, M. *Organometallics* **1992**, *11*, 2099.
(8) Farnham, W. B.; Dixon, D. A.; Middleton, W. J.; Calabrese, J. C.; Harlow, R. L.; Whitney, J. F.; Jones, G. A.; Guggenberger, L. J. *J. Am. Chem. Soc.* **1987**, *109*, 476.
(9) Corriu, R. J. P.; Kpoton, A.; Poirier, M.; Royo, G.; De Saxce, A.; Young, J. C. *J. Organomet. Chem.* **1990**, *395*, 1.
(10) Carre, F.; Corriu, R. J. P.; Kpoton, A.; Poirier, M.; Royo, G.; Young, J. C.; Belin, C. *J. Organomet. Chem.* **1994**, *470*, 43.
(11) Breliere, C.; Corriu, R. J. P.; Royo, G.; Man, M. W. C.; Zwecker, J. *C R. Acad. Sci., Ser. II Univ.* **1991**, *313*, 1527.
(12) Corriu, R. J. P.; Mazhar, M.; Poirier, M.; Royo, G. *J. Organomet. Chem.* **1986**, *306*, C5.
(13) Xie, Z.; Bau, R.; Benesi, A.; Reed, C. A. *Organometallics* **1995**, *14*, 3933.
(14) Kawai, H.; Takeda, T.; Fujiwara, K.; Suzuki, T. *J. Am. Chem. Soc.* **2005**, *127*, 12172.
(15) Takeda, T.; Kawai, H.; Fujiwara, K.; Suzuki, T. *Chem.−Eur. J.* **2007**, *13*, 7915.
(16) Wang, H.; Webster, C. E.; Perez, L. M.; Hall, M. B.; Gabbaï, F. P. *J. Am. Chem. Soc.* **2004**, *126*, 8189.
(17) Panisch, R.; Bolte, M.; Müller, T. *J. Am. Chem. Soc.* **2006**, *128*, 9676.

10.1021/om8002619 CCC: $40.75
Publication on Web 06/18/2008

Scheme 1

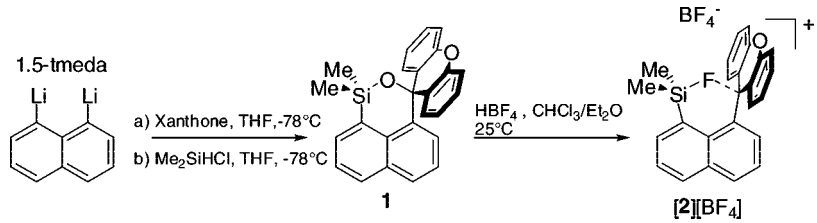

referenced against external Me_4Si (^1H, ^{13}C, ^{29}Si) and $CFCl_3$ (^{19}F). Infrared measurements were recorded on a Bruker Tensor 37 infrared spectrophotometer equipped with an ATR head.

Crystallography. Dark red single crystals could be obtained by vapor diffusion of diethyl ether into a concentrated acetonitrile solution of [**2**][BF_4]. Single crystals of **3** were obtained by crystallization from a concentrated acetonitrile solution at −20 °C. The crystallographic measurements were performed using a Bruker SMART-CCD ([**2**][BF_4]) or a Bruker APEX-II CCD (for **3**) with graphite-monochromated Mo Kα radiation (λ = 0.71069 Å). A specimen of suitable size and quality was selected and mounted onto a glass fiber with apiezon grease. The structure was solved by direct methods, which successfully located most of the non-hydrogen atoms. Subsequent refinement on F^2 using the SHELXTL/PC package (version 5.1) allowed location of the remaining non-hydrogen atoms.

Theoretical Calculations. Density functional theory (DFT) calculations (full geometry optimization) were carried out with Gaussian03 using the gradient-corrected Becke exchange functional (B3LYP) and the Lee−Yang−Parr correlation functional. A 6-31+g(d′) basis set was used for all oxygen and fluorine atoms as well as any carbon and hydrogen atoms involved in bridging interactions. A 6-31+g(d) basis set was used for silicon, and a 6-31g basis set was used for all remaining carbon and hydrogen atoms. Frequency calculations, which were carried out on the optimized structure of each compound, confirmed the absence of any imaginary frequencies. The electron density of the DFT-optimized structures of [**2**]$^+$ and **3** were subjected to an atoms-in-molecules (AIM) analysis using AIM2000. Natural bond order (NBO) analyses of the DFT-optimized geometries were visualized using the NBO View PC suite.

Synthesis of 1. A solution of xanthone (0.77 g, 4.01 mmol) in THF (20 mL) was added to a solution of 1,8-dilithionaphthalene (1.01 g, 3.90 mmol) in THF (5 mL) at −78 °C. After 30 min, addition of dimethylchlorosilane (0.50 mL, 4.50 mmol) to the resulting red-orange suspension resulted in a yellow solution, which was stirred at −78 °C for 1 h and warmed to room tempzerature. The solution was then quenched with a saturated aqueous NH_4Cl solution (15 mL), extracted with ether (2 × 15 mL), and evaporated under reduced pressure. Recrystallization from hexane yielded **1** as a pale yellow solid. Yield: 80% (1.19 g). ^1H NMR ($CDCl_3$, 400 MHz): δ 0.41 (s, 6 H, CH_{Me}), 6.91 (m, 3 H, C*H*), 7.14 (d, 2 H, CH_{Xan}, $^3J_{H-H}$ = 7.99 Hz), 7.24 (m, 5 H, C*H*), 7.58 (t, 1 H, CH_{Naph}, $^3J_{H-H}$ = 7.19), 7.74 (m, 2H, C*H*), 7.96 (d, 1 H, CH_{Naph}, $^3J_{H-H}$ = 8.39 Hz). ^{13}C NMR ($CDCl_3$, 100.5 MHz): δ 1.66, 75.48, 116.59, 123.05, 125.01, 125.29, 127.81, 128.63, 128.82, 129.62, 130.06, 130.45, 131.30, 131.69, 132.87, 134.17, 142.94, 149.08. ^{29}Si NMR ($CDCl_3$, 79.4 MHz): δ 0.03. Anal. Calcd (%) for $C_{25}H_{20}O_2Si$: C 78.91, H 5.30. Found: C 79.05, H 5.34. Melting point: 256−258 °C.

Synthesis of [2][BF_4]. Tetrafluoroboric acid (40% in H_2O, 2 mL) was added to a solution of **1** (0.50 g, 1.32 mmol) in diethyl ether (10 mL). The suspension was shaken in a separatory funnel for 10 min. The resulting deep red mixture was extracted with chloroform (2 × 10 mL). Evaporation of the resulting organic phase afforded a dark red solid, which was washed with ether (2 × 10 mL) to yield [**2**][BF_4] as a dark red air- and water-stable solid. Yield: 90% (0.55 g). ^1H NMR ($CDCl_3$, 400 MHz): δ −0.22 (d, 6 H, CH_{Me}, $^3J_{H-F}$ = 7.59 Hz), 7.61 (t, 1 H, CH_{Naph}, $^3J_{H-H}$ = 7.59 Hz), 7.73 (d, 1 H, CH_{Naph}, $^3J_{H-H}$ = 6.39 Hz), 7.79 (t, 2 H, CH_{Xan}, $^3J_{H-H}$ = 7.59 Hz), 7.83 (m, 4 H, C*H*), 8.18 (d, 1 H, CH_{Naph}, $^3J_{H-H}$ = 6.79 Hz), 8.29 (d, 1 H, CH_{Naph}, $^3J_{H-H}$ = 6.39 Hz), 8.41 (d, 2 H, CH_{Xan}, $^3J_{H-H}$ = 8.39 Hz), 8.47 (t, 2 H, CH_{Xan}, $^3J_{H-H}$ = 6.79 Hz). ^{13}C NMR ($CDCl_3$, 100.5 MHz): δ 0.51 (d, $^2J_{C-F}$ = 15.77 Hz), 120.23, 124.99 (d, $^2J_{C-F}$ = 4.52 Hz), 125.56, 126.24 (d, $^3J_{C-F}$ = 2.11 Hz), 128.99, 129.78, 131.78, 132.67, 133.46, 133.63, 134.23, 134.79, 135,17, 137.66 (d, $^3J_{C-F}$ = 5.63 Hz), 143.77, 158.55, 176.68 (d, $^1J_{C-F}$ = 6.13 Hz). ^{19}F NMR ($CDCl_3$, 375 MHz): δ −154.27 (s, $^{11}BF_4$), −154.21 (s, $^{10}BF_4$), −144.95 (sept, $^3J_{F-H}$ = 7.51 Hz). $^{29}Si\{^1H\}$ NMR ($CDCl_3$, 79.3 MHz): δ 20.3 (d, $^1J_{Si-F}$ = 286 Hz). Anal. Calcd (%) for $C_{25}H_{20}BF_5OSi$: C 63.84, H 4.29. Found: C 63.79, H 4.30. Melting point: 325−327 °C.

Synthesis of 3. Sodium borohydride (0.1 g, 2.64 mmol) was added to a solution of [**2**][BF_4] (0.75 g, 1.06 mmol) in acetonitrile (10 mL) and stirred until the red color had dissipated. The solvent was evacuated and the solid extracted with diethyl ether (3 × 10 mL). The resulting solution was concentrated and recrystallized from acetonitrile to yield **3** as a yellow crystalline solid. Yield: 70% (0.28 g). ^1H NMR ($CDCl_3$, 500 MHz): δ 0.45 (d, 6 H, CH_{Me}, $^3J_{H-F}$ = 8.49 Hz), 5.92 (s, 1 H, CH_{Xan}), 6.64 (d, 2 H, CH_{Xan}, $^3J_{H-H}$ = 7.99 Hz), 6.83 (t, 2 H, CH_{Xan}, $^3J_{H-H}$ = 6.99 Hz), 7.12 (d, 2 H, CH_{Xan}, $^3J_{H-H}$ = 8.49 Hz), 7.18 (t, 2 H, CH_{Xan}, $^3J_{H-H}$ = 7.99 Hz), 7.35 (d, 1 H, CH_{Naph}, $^3J_{H-H}$ = 6.99 Hz), 7.42 (t, 1 H, CH_{Naph}, $^3J_{H-H}$ = 7.49 Hz), 7.55 (t, 1 H, CH_{Naph}, $^3J_{H-H}$ = 8.99 Hz), 7.83 (d, 1 H, CH_{Naph}, $^3J_{H-H}$ = 7.75 Hz), 8.02 (d, 1 H, CH_{Naph}, $^3J_{H-H}$ = 7.99 Hz), 8.19 (d, 1 H, CH_{Naph}, $^3J_{H-H}$ = 6.99 Hz). ^{13}C NMR ($CDCl_3$, 125.7 MHz): δ 1.43 (d, $^2J_{C-F}$ = 17.59 Hz), 41.29 (d, $^3J_{C-F}$ = 3.01 Hz), 116.18, 122.91, 124.66 (d, $^3J_{C-F}$ = 1.50 Hz), 124.79, 126.00, 127.97, 129.32, 130.10, 131.54 (d, $^3J_{C-F}$ = 9.17 Hz), 132.19, 132.84, 134.45, 136.46 (d, $^3J_{C-F}$ = 12.19 Hz), 137.31, 143.41, 151.09. ^{19}F NMR ($CDCl_3$, 375.9 MHz): δ −148.98 (sept., $^3J_{F-H}$ = 7.89). $^{29}Si\{^1H\}$NMR ($CDCl_3$, 79.4 MHz): δ 16.42 (d, $^1J_{Si-F}$ = 276 Hz). Anal. Calcd (%) for $C_{25}H_{21}FOSi$: C 78.09, H 5.50. Found: C 78.22, H 5.51. Melting point: 190−192 °C.

Results and Discussion

Synthesis, Structure, and Properties. Reaction of 1,8-dilithionaphthalene[18] with xanthone followed by addition of chlorodimethylsilane afforded after aqueous workup the silyl ether **1**. This compound, which was isolated as a light yellow solid by recrystallization from hexane, has been characterized by NMR spectroscopy and elemental analysis. The ^1H NMR spectrum of **1** corresponds to that of a C_s-symmetrical molecule. Six resonances are detected for the unsymmetrically substituted naphthalenediyl backbone and four for the xanthene unit.

The silyl ether **1** reacts with HBF_4(aq) in a chloroform/ether mixture to afford [**2**][BF_4] as a dark red air-stable salt (Scheme 1). The $^{29}Si\{^1H\}$ NMR resonance of [**2**][BF_4] is observed as a doublet at 20.3 ppm ($^1J_{Si-F}$ = 286 Hz). Interestingly, the fluorine atom appears to be weakly interacting with the methylium carbon atom of the xanthylium moiety, whose ^{13}C NMR

(18) Neugebauer, W.; Clark, T.; Schleyer, P. v. R. *Chem. Ber.* **1983**, *116*, 3283.

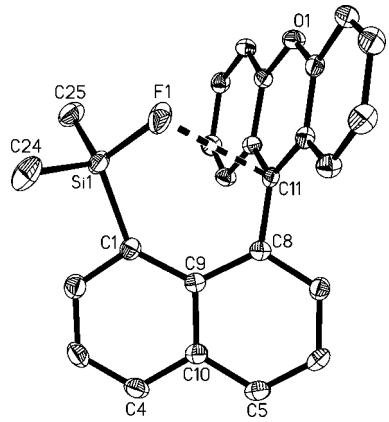

Figure 1. Crystal structure of $[\mathbf{2}]^+$ in $[\mathbf{2}][BF_4]$ (50% ellipsoids, H atoms omitted for clarity). Selected bond lengths (Å) and angles (deg): C(11)−C(8) 1.473(2), F(1)−C(11) 2.703(2), C(12)−C(11) 1.417(2), C(23)−C(11) 1.417(2), Si(1)−F(1) 1.6086(12), Si(1)−C(25) 1.839(2), Si(1)−C(24) 1.850(2), Si(1)−C(1) 1.8893(19), F(1)−Si(1)−C(25) 107.75(9), F(1)−Si(1)−C(24) 104.56(9), C(25)−Si(1)−C(24) 112.76(10), F(1)−Si(1)−C(1) 111.01(7), C(25)−Si(1)−C(1) 112.58(9), C(24)−Si(1)−C(1) 107.91(9), Si(1)−F(1)−C(11) 101.41(6), C(23)−C(11)−C(12) 118.30(14), C(23)−C(11)−C(8) 121.13(14), C(12)−C(11)−C(8) 120.48(13), C(23)−C(11)−F(1) 78.23(10), C(12)−C(11)−F(1) 89.79(11), C(8)−C(11)−F(1) 104.71(10), C(9)−C(1)−Si(1) 133.69(12), C(9)−C(8)−C(11) 123.92(15).

Table 1. Crystal Data, Data Collection, and Structure Refinement for $[\mathbf{2}][BF_4]$ and 3

	$[\mathbf{2}][BF_4]$	**3**
	Crystal Data	
formula	$C_{25}H_{20}BF_5OSi$	$C_{25}H_{21}FOSi$
M_r	470.31	384.51
cryst size (mm^3)	0.23 × 0.23 × 0.15	0.21 × 0.07 × 0.04
cryst syst	triclinic	triclinic
space group	$P\bar{1}$	$P\bar{1}$
a (Å)	9.812(2)	8.545(2)
b (Å)	10.112(2)	9.429(2)
c (Å)	13.009(3)	13.712(5)
α (deg)	110.373(4)	97.067(5)
β (deg)	105.230(4)	97.216(5)
γ (deg)	101.512(4)	115.932(3)
V ($Å^3$)	1105.4(4)	965.9(5)
Z	2	2
ρ_{calc} (g cm^{-3})	1.413	1.322
μ (mm^{-1})	0.164	0.144
$F(000)$	484	404
	Data Collection	
T (K)	110(2)	110(2)
scan mode	ω	ω
hkl range	−13 → +8	−11 → +11
	−13 → +13	−12 → +12
	−16 → +16	−17 → +15
no. of measd reflns	8873	9564
no. of unique reflns [R_{int}]	5204 [0.0245]	4458 [0.0317]
no. of reflns used for refinement	5204	4458
	Refinement	
no. of refined params	298	257
GooF	1.007	1.007
R1, wR2 all data	0.0629, 0.1576	0.0739, 0.1356
ρ_{fin}(max/min) (e $Å^{-3}$)	0.445, −0.289	0.595, −0.277

resonance is split into a doublet ($^1J_{C-F}$ = 6.13 Hz). Single crystals of $[\mathbf{2}][BF_4]$ were obtained from acetonitrile/ether and analyzed by X-ray diffraction (Figure 1, Table 1). This salt crystallizes in the $P\bar{1}$ space group with two molecules in the unit cell. Examination of the structure of the cation $[\mathbf{2}]^+$, which is well separated from the $[BF_4]^-$ anion, indicates that the fluorine atom F(1) and the methylium carbon atom C(11) are separated by 2.703(2) Å. This distance, which remains within the sum of the van der Waals radii of the two elements (r_{vdw}(F) = 1.30−1.38 Å, r_{vdw}(C) = 1.7 Å),[19,20] is longer than the F → C distance of 2.444(2) Å observed in $[\mathbf{II}]^+$ and can only correspond to a very weak interaction.[16] Moreover, the structure of $[\mathbf{2}]^+$ presents a number of features characteristic of sterically strained *peri*-substituted naphthalene derivatives. The core of the naphthalene backbone is twisted, as reflected by the dihedral angle θ of 4.5° formed between the planes defined by C(1)−C(9)−C(8) and C(4)−C(10)−C(5); the C(9)−C(1)−Si(1) (133.69(12)°) and C(9)−C(8)−C(11) (123.92(15)°) angles substantially deviate from the ideal value of 120°, thus suggesting that the F(1)−C(11) interaction is enforced by the rigid naphthalenediyl linker. In agreement with the weakness of this interaction, we note that the methylium carbon atom C(11) retains a formal sp^2 hybridization, as indicated by its trigonal-planar geometry ($\sum_{(C-C(11)-C)}$ = 359.91°). The Si(1)−F(1) bond of 1.609(1) Å shows no lengthening when compared to other dimethylarylfluorosilanes.[21]

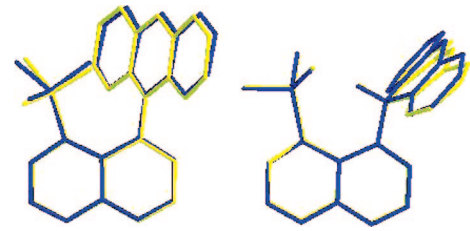

Figure 2. Overlays of the experimental (yellow) and calculated (blue) structures of $[\mathbf{2}]^+$ (left) and **3** (right) viewed perpendicular to the naphthalene ring.

The DFT-optimized structure corresponds closely with that experimentally determined (Figure 2). The F(1)−C(11) distance of 2.66 Å is similar to that observed in the crystalline geometry. An AIM analysis of this interaction reveals a bond path between the F(1) and the C(11) atoms with an electron density $\rho(r)$ of 1.56 × 10^{-2} e $bohr^{-3}$ at the bond critical point (BCP) (Figure 3). This value, which is much lower than the $\rho(r)$ of 2.16 × 10^{-2} e $bohr^{-3}$ computed for $[\mathbf{II}]^+$, confirms the weakness of the interaction. However, an NBO analysis of the molecule indicates overlap of the empty p_z-orbital of C(11) with a lone pair (lp) localized in a 2p-orbital on F(1), an interaction similar to the F → C interaction described for $[\mathbf{II}]^+$.

Reduction of $[\mathbf{2}][BF_4]$ with $NaBH_4$ in acetonitrile leads to formation of **3** (Scheme 2). Compound **3** has been isolated as an air-stable solid in 70% yield. The appearance of a singlet in the ^1H NMR spectrum of **3** at 5.92 ppm provides clear spectroscopic evidence for the presence of a hydride bound to the former methylium center of the xanthene moiety. ^{29}Si NMR spectroscopy indicates that this hydride is not coupled to the silicon nucleus. Nevertheless, when compared to $[\mathbf{2}][BF_4]$, the $^{29}Si\{^1H\}$ NMR resonance of **3** at 16.4 ppm is shifted slightly upfield, which could be consistent with an increase in the coordination number of the silicon center.[22,23] This view is supported by a measurable change of the $^1J_{Si-F}$, which decreases from 286 Hz in $[\mathbf{2}][BF_4]$ to 276 Hz in **3**. Furthermore, comparing

(19) Nyburg, S. C.; Faerman, C. H. *Acta Crystallogr., Sect. B: Struct. Sci.* **1985**, *B41*, 274.
(20) Caillet, J.; Claverie, P. *Acta Crystallograph., Sect. A* **1975**, *31*, 448.
(21) Grobe, J.; Martin, R.; Krebs, B.; Henkel, G. *Z. Anorg. Allg. Chem.* **1992**, *607*, 131.
(22) Breliere, C.; Corriu, R. J. P.; Royo, G.; Zwecker, J. *Organometallics* **1989**, *8*, 1834.
(23) Akkari-El Ahdab, A.; Rima, G.; Gornitzka, H.; Barrau, J. *J. Organomet. Chem.* **2001**, *636*, 96.

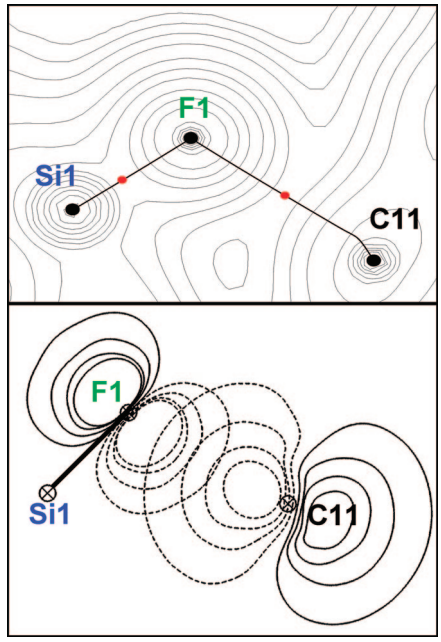

Figure 3. Top: AIM contour plot of the electron density of $[\mathbf{2}]^+$ shown in the Si−F−C plane along with bond paths and critical points. Bottom: NBO contour plot showing the $lp_{(F)} \rightarrow p_{z(C)}$ interaction.

Scheme 2

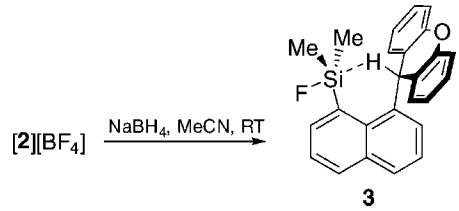

the IR stretching frequency of the central C−H bond of **3** (2928 cm^{-1}) with that of 9-(naphthalen-1-yl)-9*H*-xanthene (2937 cm^{-1}) indicates a weakening by 9 cm^{-1}, which could be assigned to a C−H → Si interaction.

Single crystals of **3** were grown from acetonitrile and analyzed by X-ray diffraction (Figure 4, Table 1). The former methylium center C(11) is tetrahedral ($\Sigma_{(C-C(11)-C)} = 333.2°$). It is bound to the H(1) hydrogen atom, which was located on the difference map and refined isotropically. According to this X-ray measurement and in good agreement with theoretical calculations (*vide infra*), the hydrogen atom H(1) is located only 2.32(2) Å away from the Si(1) silicon atom, which is well within the sum of the van der Waals radii of the two elements (ca. 3.1 Å).[24] This Si−H distance is shorter than the Si−H separation of 2.73 Å found in $[Mes_3Si]^+$[25] but longer than those sometimes observed in main group or transition metal complexes with silicon hydride bridges.[17,24,26–32] The Si(1)−H(1) distance can also be compared to the 2.12−2.39 Å range observed for the CH → C distance

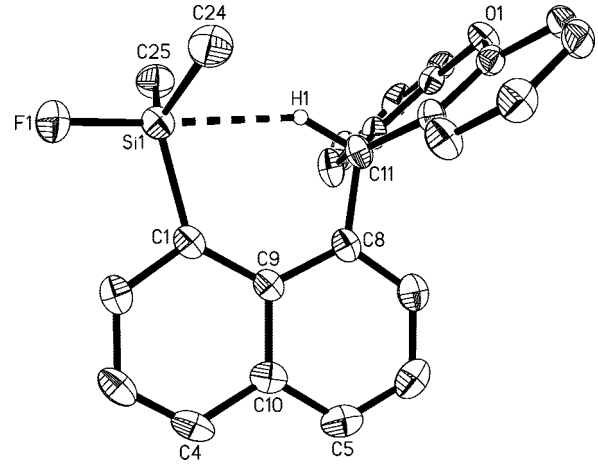

Figure 4. Crystal structure of **3** (50% ellipsoids, H atoms omitted for clarity). Selected bond lengths (Å) and angles (deg): Si(1)−F(1) 1.6229(14), Si(1)−C(24) 1.846(2), Si(1)−C(25) 1.847(2), Si(1)−C(1) 1.896(2), Si(1)−H(1) 2.32(2), C(11)−H(1) 1.11(2), C(11)−C(8) 1.519(3),C(11)−C(23)1.520(3),C(11)−C(12)1.524(3),F(1)−Si(1)−C(24) 102.47(10), F(1)−Si(1)−C(25) 102.67(9), C(24)−Si(1)−C(25) 114.69(11), F(1)−Si(1)−C(1) 103.85(8), C(24)−Si(1)−C(1) 116.66-(10), C(25)−Si(1)−C(1) 113.92(10), F(1)−Si(1)−H(1) 177.0(5), C(24)−Si(1)−H(1) 75.3(5), C(25)−Si(1)−H(1) 76.8(5), C(1)−Si-(1)−H(1) 79.0(5), H(1)−C(11)−C(8) 110.0(10), H(1)−C(11)−C(23) 108.0(10), C(8)−C(11)−C(23) 111.69(17), H(1)−C(11)−C(12) 105.5(10), C(8)−C(11)−C(12) 110.94(16), C(23)−C(11)−C(12) 110.56(16), C(9)−C(1)−Si(1) 132.55(15), C(9)−C(8)−C(11) 124.56(19).

of cations $[\mathbf{Ia}-\mathbf{c}]^+$.[14,15] Another conspicuous feature concerns the F(1)−Si(1)−H(1) angle of 177.0(5)°, which indicates that the hydrogen atom occupies an axial coordination site directly opposite the fluorine atom. In agreement with this view, we note (i) a slight elongation of the Si(1)−F(1) bond (1.623(1) vs 1.609(1) Å in $[\mathbf{2}]^+$) and (ii) a substantial increase in the sum of the C−Si(1)−C angles on going from $[\mathbf{2}]^+$ to **3** ($\Sigma_{(C-Si1-C)} =$ 345.27° in **3** vs 333.2° in $[\mathbf{2}]^+$). While the values of the C(9)−C(1)−Si(1) (132.55(15)°) and C(9)−C(8)−C(11) (124.56-(19)°) angles are similar to those measured in $[\mathbf{2}]^+$, the naphthalene backbone of **3** is twisted by an angle θ of only 1.0°, indicating less steric crowding. Altogether, these structural results indicate the presence of a C−H → Si agostic interaction in **3**. To our knowledge, such interactions are unprecedented in the chemistry of fluorosilanes but have been observed in electrophilic silicon species such as $[i\text{-}Pr_3Si]^+$, which forms an α-C−H agostic interaction.[13]

The DFT-optimized structure corresponds closely with that experimentally determined (Figure 2). In particular, the Si(1)−H(1) separation of 2.32 Å is close to that observed in the crystal. AIM calculations, which have proved useful for the characterization of agostic interactions in d^0 metal alkyl complexes,[33] show the presence of a bond path between the Si(1) and the H(1) atoms with an electron density $\rho(r)$ of 1.68 × 10^{-2} e $bohr^{-3}$ at the BCP (Figure 5). This value, which is much weaker than those computed for the Si−H bonds of $PhMe_2SiH$ of 11.53 × 10^{-2} e $bohr^{-3}$ and $[\mathbf{III}]^+$ (av 7.44 × 10^{-2} e $bohr^{-3}$), reveals the presence of a relatively weak interaction. Nevertheless, its presence can be further asserted through an NBO

(24) Gountchev, T. I.; Tilley, T. D. *J. Am. Chem. Soc.* **1997**, *119*, 12831.
(25) Kim, K.-C.; Reed, C. A.; Elliott, D. W.; Mueller, L. J.; Tham, F.; Lin, L.; Lambert, J. B. *Science* **2002**, *297*, 825.
(26) Khalimon, A. Y.; Lin, Z. H.; Simionescu, R.; Vyboishchikov, S. F.; Nikonov, G. I. *Angew. Chem., Int. Ed. Engl.* **2007**, *46*, 4530.
(27) Hoffmann, S. P.; Kato, T.; Tham, F. S.; Reed, C. A. *Chem. Commun.* **2006**, 767.
(28) Sekiguchi, A.; Murakami, Y.; Fukaya, N.; Kabe, Y. *Chem. Lett.* **2004**, *33*, 530.
(29) Müller, T. *Angew. Chem., Int. Ed. Engl.* **2001**, *40*, 3033.
(30) Nikonov, G. I.; Kuzmina, L. G.; Lemenovskii, D. A.; Kotov, V. V. *J. Am. Chem. Soc.* **1995**, *117*, 10133.
(31) Schubert, U.; Ackermann, K.; Woerle, B. *J. Am. Chem. Soc.* **1982**, *104*, 7378.
(32) Nikonov, G. I. *Adv. Organomet. Chem.* **2005**, *53*, 217.
(33) Scherer, W.; McGrady, G. S. *Angew. Chem., Int. Ed. Engl.* **2004**, *43*, 1782.

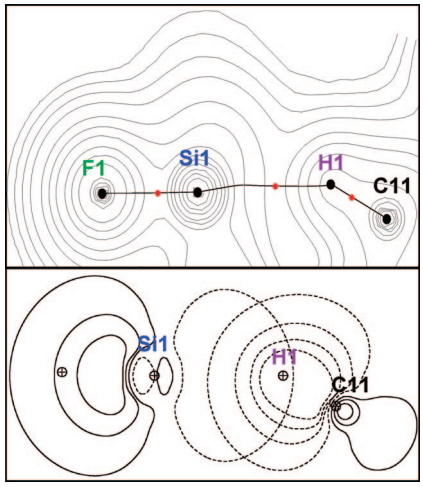

Figure 5. Top: AIM contour plot of the electron density of **3** shown in the F(1)−Si(1)−H(1)−C(11) plane along with bond paths and critical points. Bottom: NBO contour plot showing the $\sigma_{(C-H)} \rightarrow p_{z(Si)}$ interaction.

analysis performed at the B3LYP-optimized geometry. This analysis identifies a donor−acceptor interaction involving the C−H σ-bond as a donor and the silicon empty p_z-orbital as the acceptor. It is also important to note that this NBO analysis describes the Si−F bond as a donor−acceptor interaction involving a fluorine lone pair as the donor and the silicon empty p_z-orbital as the acceptor. Hence, the silicon center in **3** bears the bonding characteristic of a five-coordinate silicon species such as $[PhSiMe_2F_2]^-$ where both axial fluoride ligands compete for a unique silicon p-orbital.[34] Further insights into the nature of the interaction were gained from a computational survey of a series of molecules in which the fluorine atom of **3** is substituted by a group X (X = CH_3, NH_2, OH). As shown in Table 2, the Si(1)−H(1) distance decreases as the Lewis acidity of the silicon center increases. This shortening is also accompanied by an increase of $\rho(r)$ at the BCP. These computational results further substantiate the presence of a donor−acceptor $R_3C-H \rightarrow SiFR_3$ interaction in **4**. Lastly, a deletion calculation carried out by zeroing the Kohn−Sham matrix elements

(34) NBO analysis of $[PhSiMe_2F_2]^-$ at the B3LYP geometry indicates that the fluoride ligands are bound to the silicon center via donor−acceptor interactions similar to those in **3**. See the Supporting Information.

Table 2. Computed Metrical Parameters and Electron Density for Molecules 3 and 4X

Cpd	Si(1)-H(1) (Å)	$\Sigma_{(C-Si-C)}$ (°)	$\rho(r)$@BCP (e bohr^{-3})
4CH_3	2.40	340.2	1.55×10^{-2}
4NH_2	2.40	340.9	1.52×10^{-2}
4OH	2.36	343.7	1.60×10^{-2}
3	2.32	346.8	1.68×10^{-2}

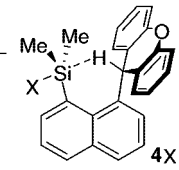

corresponding to the $\sigma_{(C-H)} \rightarrow p_{z(Si)}$ interaction leads to an increase of the total energy of the molecule by 3.069 kcal/mol. This deletion calculation suggest that the $\sigma_{(C-H)} \rightarrow p_{z(Si)}$ interaction is comparable in energy to a moderately strong hydrogen bond.[35] This interaction is weaker than classical agostic interactions because of the absence of back-bonding.

Conclusion

In conclusion, we report the synthesis and structural characterization of a compound featuring an agostic $R_3C-H \rightarrow SiFR_3$ interaction. Formation of this interaction is made possible by the use of the naphthalene backbone, which holds the interacting functionalities in close proximity. Despite its weakness, the presence of this interaction is indubitable and notably affects the geometry of the silicon center, which adopts a distorted trigonal-bipyramidal geometry.

Acknowledgment. This work was supported by the National Science Foundation, (CHE-0646916), Welch Foundation (A-1423), and the Petroleum Research Funds administered by the American Chemical Society (44832-AC4).

Supporting Information Available: Geometries of the computed structures and X-ray crystallographic data in CIF format. This material is available free of charge via the Internet at http://pubs.acs.org.

OM8002619

(35) Vorobyov, I.; Yappert, M. C.; DuPre, D. B. *J. Phys. Chem. A* **2002**, *106*, 668.